ELSEVIER

Journal of Molecular Catalysis A: Chemical 195 (2003) 63–82

JOURNAL OF MOLECULAR CATALYSIS A: CHEMICAL

www.elsevier.com/locate/molcata

^{31}P NMR and IR characterization of enantioselective olefin and arene hydrogenation catalysts containing a rhodium–chiral phosphine complex tethered on silica

Keith J. Stanger, Jerzy W. Wiench, Marek Pruski, Robert J. Angelici*

Ames Laboratory and Department of Chemistry, Iowa State University, Ames, IA 50011-3111, USA

Received 20 May 2002; received in revised form 7 October 2002

Abstract

Rhodium complexes of the chiral chelating phosphine (2*S*,4*S*)-4-(diphenylphosphino)-2-(diphenylphosphinomethyl)pyrrolidine (X-PPM) tethered on silica (SiO_2), tethered on silica with supported palladium (Pd-SiO_2), and in solution were characterized by ^{31}P NMR and IR spectroscopies. These studies show that the (X-PPM)Rh(COD)$^+$ complex, which is highly enantioselective for the hydrogenation of the prochiral olefin methyl-α-acetamidocinnamate (MAC), retains its composition in the tethered catalysts regardless of its mode of preparation or the presence of Pd on the silica surface. These investigations also show that the chiral diphosphine ligand remains coordinated to the rhodium during the reaction. Both the tethered and solution catalysts are moderately air sensitive prior to use, giving the free phosphine oxide of X-PPM, which is no longer coordinated to the rhodium. During and after use in catalytic reactions, the tethered rhodium complexes are extremely air-sensitive, but were characterized by ^{31}P NMR and IR spectra of their carbon monoxide derivatives. Finally, the catalysts were examined for their arene hydrogenation activity. It was established that Pd in the (X-PPM)Rh(COD)$^+$/Pd-SiO_2 catalyst causes the reduction of any uncomplexed Rh to metallic species during the hydrogenation reactions. It was these metallic Rh species that were responsible for the toluene hydrogenation activity of these tethered (X-PPM)Rh(COD)$^+$/Pd-SiO_2 catalysts.

Keywords: Immobilized metal catalysts; Enantioselective olefin hydrogenation; Rhodium; Solid state ^{31}P-NMR; Arene hydrogenation; Silica; Palladium

1. Introduction

There is currently much interest in the synthesis of chiral organic compounds using enantioselective transition metal catalysts for the hydrogenation of prochiral olefins [1–4]. Within this methodology, the use of chiral phosphine–metal complexes represents an effective and highly studied area [1–4]. When such enantioselective catalysts are tethered on solid supports, the resulting catalysts combine the advantages of both homogeneous (selectivity, tuneability, and homogeneous sites) and heterogeneous (recovery and separation) catalysts [1–3]. Therefore, the immobilization of enantioselective homogeneous catalysts is a highly desirable goal.

One of the best examples of an immobilized enantioselective hydrogenation catalyst is that reported by Pugin and Müller [5] and Pugin [6] who

* Corresponding author.
E-mail addresses: mpruski@iastate.edu (M. Pruski), angelici@iastate.edu (R.J. Angelici).

1381-1169/02/$ – see front matter © 2002 Elsevier Science B.V. All rights reserved.
PII: S1381-1169(02)00572-1

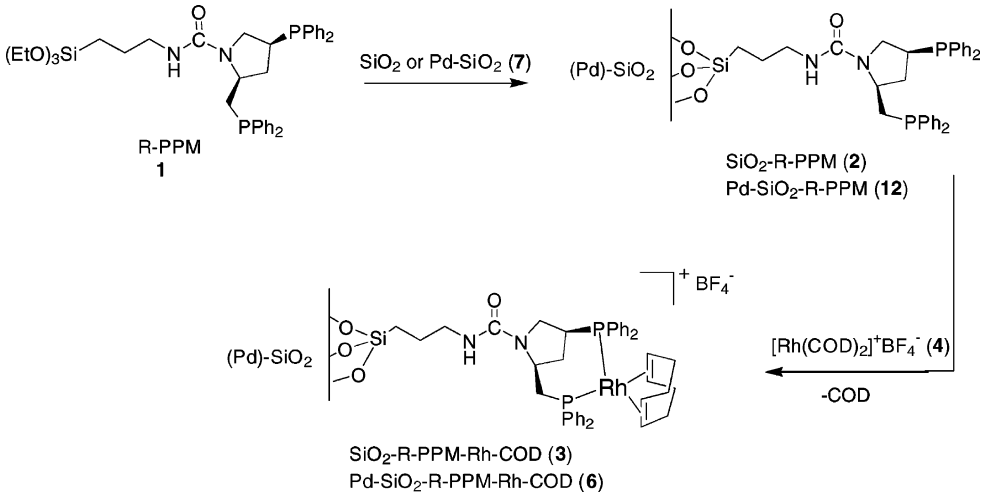

Scheme 1. Preparation of the tethered catalysts SiO_2-*R*-PPM-Rh-COD (**3**B) and Pd-SiO_2-*R*-PPM-Rh-COD (**6**B) using Method B.

examined the enantioselective hydrogenation of methyl-α-acetamidocinnamate, MAC, Eq. (1),

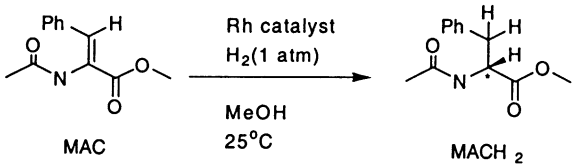

(1)

using rhodium catalysts containing the chiral chelating phosphine (2*S*,4*S*)-4-(diphenylphosphino)-2-(diphenylphosphinomethyl)pyrrolidine, PPM, Eq. (2),

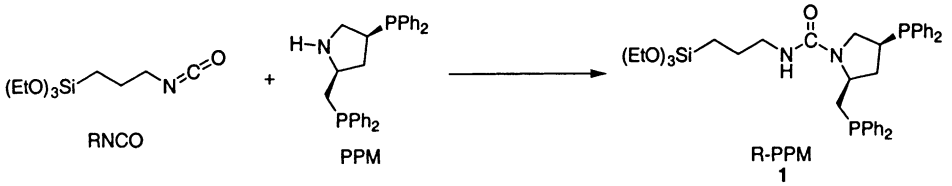

(2)

tethered on silica. The catalysts were prepared as shown in Scheme 1. The addition of $[Rh(COD)_2]^+BF_4^-$ (**4**), where COD = 1,5 cyclooctadiene, to the immobilized chiral, bidentate PPM ligand produced a very active and highly enantioselective catalyst SiO_2-*R*-PPM-Rh-COD (**3**), with activities and enantioselectivities comparable to those of the untethered $[(B\text{-}PPM)Rh(COD)]^+BF_4^-$ (**5**) (B = $-CO_2(t\text{-}Bu)$) in solution, with turnover frequencies (TOF) of 6.25–12.5 min^{-1} and enantiomeric excesses (ees) of 89.8–94.5% [5].

In previous studies from our group [7–11], we observed that rhodium complexes immobilized on silica that also contained supported palladium metal were highly active catalysts for the hydrogenation of arenes. Given the high enantioselectivity of Pugin's SiO_2-*R*-PPM-Rh-COD (**3**) catalyst, we sought to determine whether this catalyst in combination with supported Pd metal would serve as an enantioselective catalyst for the hydrogenation of prochiral arenes.

Prior to performing the arene hydrogenation studies, we sought to characterize the SiO_2-*R*-PPM-Rh-COD (**3**) catalyst and to understand its stability especially with respect to air oxidation. These studies, together with initial investigations of arene hydrogenation using Pd-SiO_2-*R*-PPM-Rh-COD (**6**), consisting of SiO_2-*R*-PPM-Rh-COD (**3**) and supported Pd metal, are described in this paper. These catalysts were investigated by ^{31}P NMR spectroscopy, diffuse reflectance infrared Fourier transform (DRIFT) spectroscopy, reaction studies (including measurements

of rates and enantioselectivities of hydrogenation reactions), and mercury metal poisoning experiments.

2. Experimental

2.1. General considerations

The chemicals $RhCl_3 \cdot 3H_2O$ (Pressure Chemicals), $PdCl_2$ (DFG), 3-isocyanatopropyltriethoxysilane RNCO (Fluka), H_2O_2 (30 wt.%), PPM, and COD (Aldrich) were purchased from commercial sources and used as received. Silica gel Merck grade 10184 (BET surface area, $300\,m^2\,g^{-1}$; pore size 100 Å) (Aldrich) was dried under vacuum at 150 °C for 12 h and kept under argon before use. Toluene and methylene chloride were dried prior to use by passage through an alumina column under argon [12]. Methanol was distilled from Mg/I_2 under nitrogen [13]. The preparation of MAC followed a literature procedure [14,15] that utilized methanolysis of *Z*-methyl-4-benzaloxazolone [15]. Purification of MAC was achieved by repeated recrystallization from MeOH. The compound $[Rh(COD)_2]^+BF_4^-$ (**4**) was prepared by the general procedures reported by Schrock and Osborn [16]. The preparation of Pd-SiO_2 (10% Pd w/w) (**7**) [17,18] was described previously. All manipulations involving rhodium or phosphine were carried out under an argon atmosphere using standard Schlenk techniques.

FTIR and DRIFT spectra were obtained on a Nicolet 560 spectrophotometer. The main compartment, equipped with a TGS detector and an NaCl solution cell, was used to take solution IR spectra. An auxiliary experiment module (AEM) containing a Harrick diffuse reflectance accessory with a MCT detector was used to obtain the DRIFT spectra of solid samples. Gas chromatographic (GC) analyses were performed on a Hewlett Packard HP 6890 GC using a 25 m HP-1 capillary column and an FID (flame ionization detector). Enantiomeric excesses were determined by GC analysis of products on a Chirasil-Val capillary column (50 m × 250 μm) (Alltech) capable of separating the two enantiomers of the hydrogenation product *N*-acetyl-phenylalanine methyl ester, $MACH_2$ (**8**). GC samples were taken from the reaction mixtures and either run as obtained or diluted with ethanol as necessary.

^{31}P NMR spectra of liquid samples were run at 161.92 MHz on a Bruker DRX 400-MHz NMR spectrometer. ^{31}P solid-state NMR spectra were carried out at the same frequency using a Chemagnetics CMX Infinity spectrometer equipped with a 3.2 mm magic angle spinning (MAS) probe. The MAS rotors were loaded in a glove bag under dry nitrogen to reduce oxidation of samples during the experiments. The relaxation measurements yielded T_1 values of at least 300 s for ^{31}P and 1 to 3 s for ^1H. Thus, cross polarization (CP) between ^1H and ^{31}P was applied in order to enhance the sensitivity and reduce the recycle delay between consecutive scans. The experiments used a cosine-modulated CP scheme synchronized with the rotor period [19], using a sample rotation rate of 18 kHz (unless specified otherwise), contact time of 0.5 ms, continuous wave ^1H decoupling at 70 kHz, pulse delay of 5 s and number of scans between 128 and 8000. All phosphorus chemical shifts are reported using the δ scale, with positive values being downfield, and are referenced to an 85% solution of H_3PO_4 in water.

Rhodium content of the supported catalysts was determined by ICP-AES conducted by MPC Analytical Services of the Ames Laboratory. Samples for analysis were prepared by dissolving a 50 mg of the supported catalyst in 5.0 ml of aqua regia at 90 °C; then 5.0 ml of 5% aqueous HF was added and the mixture was heated to the same temperature. The resulting solution was diluted to 25 ml in a volumetric flask. For the catalysts prepared by Method A, the average rhodium loadings on SiO_2 were 79% (78.9±9.4) of the rhodium added; those on Pd-SiO_2 were 70% (69.9 ± 10.5) of the rhodium added. For the catalysts prepared by Method B or by adsorbing the Rh complexes on SiO_2 or Pd-SiO_2, the rhodium added to the system corresponds to the rhodium present (as no washings precede catalyst use). The experimentally determined rhodium compositions were used in the rate (TOF) calculations.

2.1.1. Preparation of rhodium complexes

*2.1.1.1. PPM-Rh-COD (**9**).* A mixture of 15.0 mg (33.1 μmol) of PPM and 13.4 mg (33.0 μmol) of $[Rh(COD)_2]^+BF_4^-$ (**4**) dissolved in 1.0 ml of degassed CH_2Cl_2 or $CDCl_3$ was stirred under argon for 15 min. The ^{31}P NMR spectrum of (**9**) in $CDCl_3$ is very similar to that reported in the literature for the

same complex with another counter anion (ClO_4^-) [20]: δ 42.4 (d of d, $J_{Rh-P} = 113$ Hz, $J_{P-P} = 37$ Hz) and 32.5 (d of d, $J_{Rh-P} = 110$ Hz, $J_{P-P} = 37$ Hz).

*2.1.1.2. R-PPM (**1**).* Compound **1** was prepared in a manner similar to that described in the literature [5]. Solid PPM, 15.0 mg (33.1 μmol), dissolved in 1.0 ml of CH_2Cl_2 was treated with 9.1 μl (37 μmol, 1.2 eq.) of RNCO and stirred for 20 min. The procedure worked equally well in toluene or $CDCl_3$. The resulting solution of *R*-PPM (**1**) was used directly for complexation to rhodium or tethering to silica. Spectral data are identical to those reported in the literature [5]. ^{31}P NMR ($CDCl_3$): δ −8.2 (s) and −22.3 (s).

*2.1.1.3. R-PPM-Rh-COD (**10**).* The preparation of the phosphine–rhodium complex *R*-PPM-Rh-COD (**10**) was similar to that for analogous Rh(diphosphine)(COD)$^+$ complexes reported in the literature [3,20–23]. A CH_2Cl_2 or $CDCl_3$ solution of 9.6 mg (14 μmol) of *R*-PPM (**1**) in 0.7 ml of solvent was added to 5.0 mg (12 μmol, 0.9 eq.) of $[Rh(COD)_2]^+BF_4^-$ (**4**) and stirred for 10 min. The resulting product **10** was isolated by removal of solvent under vacuum, washing with hexanes (3 ml × 1 ml), and drying under vacuum. ^{31}P NMR ($CDCl_3$): δ 44.2 (d of d, $J_{Rh-P} = 146$ Hz, $J_{P-P} = 38$ Hz) and 16.8 (d of d, $J_{Rh-P} = 140$ Hz, $J_{P-P} = 38$ Hz).

2.1.2. Preparation of silica-tethered complexes

*2.1.2.1. SiO_2-R-PPM (**2**).* Following a general procedure for tethering trialkoxysilanes to silica surfaces [7], 23.2 mg (33.1 μmol) of *R*-PPM (**1**) was dissolved in 3.0 ml of toluene and slurried over 0.12 g of SiO_2. The mixture was stirred at reflux for 12 h and then cooled to RT and stirred overnight. The resulting solid was washed three times with 5.0 ml of toluene and then

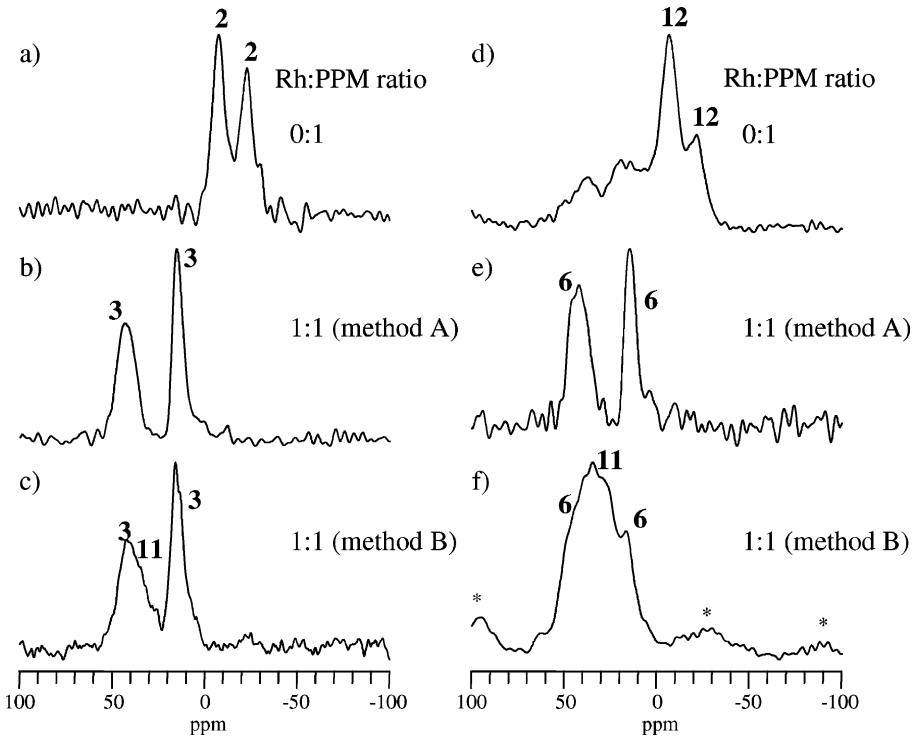

Fig. 1. ^{31}P CPMAS NMR spectra of (a) chiral phosphine SiO_2-*R*-PPM (**2**); (b), (c) SiO_2-*R*-PPM-Rh-COD (**3**) complex prepared by Methods A and B, respectively; (d) Chiral phosphine Pd-SiO_2-*R*-PPM (**12**); (e), (f) Pd-SiO_2-*R*-PPM-Rh-COD (**6**) complex prepared by Methods A and B, respectively. Spectrum (f) was acquired using a lower spinning rate of 10 kHz. Asterisks (∗) denote the spinning sidebands.

dried under vacuum. ^{31}P CPMAS NMR (Fig. 1a): δ −7 and −23 ppm.

*2.1.2.2. SiO_2-R-PPM-Rh-COD (**3**). Method A*: A solution of 53.5 mg (53.6 μmol) of *R*-PPM-Rh-COD (**10**) dissolved in 5.0 ml of methylene chloride/toluene (1:4) solution was added to 0.20 g of SiO_2. The resulting slurry was refluxed for 12 h and then stirred overnight at room temperature. Filtration, followed by washing with 5.0 ml of CH_2Cl_2 three times, and drying under vacuum gave **3**A. *Method B*: Following the preparation described by Pugin and Müller [5], a 1.0 ml MeOH solution containing 9.9 mg (24.4 μmol) of $[Rh(COD)_2]^+BF_4^-$ (**4**) was added to 0.10 g (∼26 μmol of *R*-PPM (**1**), based on initial loading) of SiO_2-*R*-PPM (**2**). The resulting solid **3**B was then dried under vacuum. Both methods produced nearly identical surface species as determined by solid-state ^{31}P NMR spectroscopy. ^{31}P CPMAS NMR (Fig. 1b and c): δ 43 and 15 ppm.

*2.1.2.3. SiO_2-R-PPM-O_2 (**11**).* The tethered phosphine oxide **11** was produced by three methods: (a) a slurry of 50 mg of SiO_2-*R*-PPM (**2**) in 2.0 ml of acetone was treated with five drops of H_2O_2 (30 wt.%) and stirred for 15 min. The solid was dried under vacuum. (b) A slurry of 50 mg of SiO_2-*R*-PPM-Rh-COD (**3**) in 2.0 ml of acetone was reacted with 5 drops of H_2O_2 (30 wt.%) for 15 min. The solid was dried under vacuum. (c) A vial of 50 mg of SiO_2-*R*-PPM-Rh-COD (**3**) was exposed to ambient atmosphere for 5 days. All three methods gave the same product (**11**), although some starting material (**3**) was observed in Method (c) after only 3 days. ^{31}P CPMAS NMR (Fig. 2): δ 35 ppm.

2.1.3. Preparation of tethered complexes on palladium silica gel

*2.1.3.1. Pd-SiO_2-R-PPM (**12**).* Similar to the preparation of SiO_2-*R*-PPM (**2**), a solution of 23.2 mg (33.1 μmol) of *R*-PPM (**1**) in 3.0 ml of toluene was slurried with 0.12 g of Pd-SiO_2 (**7**). The mixture was stirred at reflux for 12 h and then cooled to room temperature and stirred overnight. The resulting solid was washed three times with 5.0 ml of toluene and then dried under vacuum. ^{31}P CPMAS NMR (Fig. 1d): δ −7 and −21 ppm.

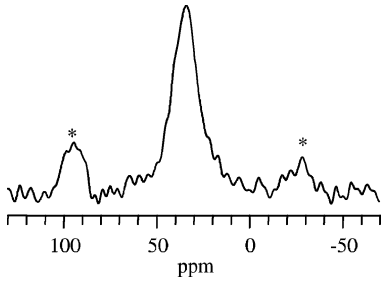

Fig. 2. ^{31}P CPMAS NMR spectrum of SiO_2-*R*-PPM-O_2 (**11**) obtained using a sample rotation rate of 10 kHz. Asterisks (∗) denote the spinning sidebands.

*2.1.3.2. Pd-SiO_2-R-PPM-Rh-COD (**6**). Method A*: A solution of 53.5 mg (53.6 μmol) of *R*-PPM-Rh-COD (**10**) dissolved in 5.0 ml of methylene chloride/toluene (1:4) was added to 0.20 g of Pd-SiO_2 (**7**). The resulting slurry was refluxed for 12 h and then stirred overnight at room temperature. Filtration, followed by washing three times with 5.0 ml of CH_2Cl_2 and drying under vacuum gave **6**A. *Method B*: A solution consisting of 9.9 mg (24.4 μmol) of $[Rh(COD)_2]^+BF_4^-$ (**4**) in 1.0 ml of MeOH was added to 0.10 g (26.8 μmol *R*-PPM) of Pd-SiO_2-*R*-PPM (**12**). The resulting solid **6**B was then dried under vacuum. Method A produced the expected surface species, **6**, as established by solid-state ^{31}P NMR spectroscopy (see the ^{31}P CPMAS spectrum of Fig. 1e with two resonances at 45 and 15 ppm). In the corresponding ^{31}P CPMAS spectrum of the sample prepared using Method B, the resonances at 45 and 15 ppm are superimposed with additional lines centered at around 35 ppm for the phosphine oxide **13** (see Fig. 1f).

*2.1.3.3. Pd-SiO_2-R-PPM-O_2 (**13**).* The tethered phosphine oxide on Pd-SiO_2 **13** was produced by three methods: (a) A slurry of 50 mg of Pd-SiO_2-*R*-PPM (**12**) in 2.0 ml of acetone was treated with five drops of H_2O_2 (30 wt.%) and stirred for 15 min. The solid was dried under vacuum. (b) A slurry of 50 mg of Pd-SiO_2-*R*-PPM-Rh-COD (**6**) in 2.0 ml of acetone was reacted with five drops of H_2O_2 (30 wt.%) for 15 min. The solid was dried under vacuum. (c) A vial of 50 mg of Pd-SiO_2-*R*-PPM-Rh-COD (**6**) was exposed to ambient atmosphere for 5 days. Again, for all three methods, the product (**13**) was identical, although starting

material (**6**) was observed after only 3 days in method (c). ^{31}P CPMAS NMR: δ 35 ppm (the same as Fig. 2).

2.1.4. Hydrogenation reactions

2.1.4.1. Hydrogenation of MAC. A standard hydrogenation run consisted of placing 50 mg of catalyst (∼13.4 μmol of Rh) into a three-necked, jacketed vessel containing a Teflon-coated stir bar. One neck of the reaction vessel was capped with a glass stopper. The center neck was fitted with a rubber and Teflon septum to allow for input of solvents and removal of GC samples via syringe. The third neck was fitted with a three arm "Y" stopcock. This allowed the reaction vessel to be attached to a vacuum/argon Schlenk line and a burette filled with hydrogen. After the catalyst was placed in the reaction vessel, the atmosphere in the reaction flask was replaced with Ar using three vacuum/flush cycles. Next, the jacket of the vessel was attached to a constant temperature bath and the temperature was raised to 25.0 ± 0.2°C. While the temperature was being achieved, the hydrogen gas reservoir was filled though a series of three consecutive vacuum and hydrogen gas flush cycles. After the temperature had stabilized at 25.0 °C and the gas burette was full of hydrogen, the reaction vessel itself was evacuated and filled with hydrogen three times. Immediately after replacing the Ar atmosphere with hydrogen, 5.0 ml of a 0.10 M MAC solution in MeOH were added via syringe. The reaction was opened to the hydrogen gas reservoir, stirring was initiated, and hydrogen uptake was recorded. The rate of reaction was monitored by the volume of hydrogen taken up with time. In addition, conversions based on H_2 uptake were confirmed by GC analysis of the solutions during and after the reaction. In all cases, $MACH_2$ (**8**) was the only MAC-hydrogenation product observed by GC, and the hydrogen uptake reading from the burette matched the GC analysis.[1]

2.1.4.2. Hydrogenation of toluene. The general procedure used for the hydrogenation of MAC was employed with the following modifications: the temperature of the reaction was held at 40.0 ± 0.2°C, and the solvent (toluene) was also the reactant.

2.1.4.3. Mercury poisoning studies. The general procedure used for the hydrogenation of MAC or toluene was employed with the following modification: 0.10 ml (6.8 mmol, ∼10 eq. compared to Rh) of Hg was added prior to or after solvent addition.

2.1.4.4. Catalyst reuse. Two methods of catalyst reuse were examined. The first consisted of filtering the reaction mixture, washing the solid catalyst with MeOH, drying it, and reweighing it. This inevitably exposed the used catalyst to the atmosphere during the reweighing step. The air sensitivity of the catalyst during and after reaction results in deactivation of the catalyst if it is exposed to air even for a few seconds and prevents reuse by this method. The second method of catalyst reuse involved the in situ addition of extra MAC substrate, without isolation of the used catalyst from the reaction vessel. In this case, the catalyst retained its activity when additional substrate, MAC, was added to the reaction vessel.

3. Results and discussion

3.1. Characterization of the catalyst and its components before hydrogenation of MAC

3.1.1. Characterization of X-PPM and (X-PPM)Rh(COD)$^+$ species in solution

The parent PPM and *R*-PPM complexes in solution serve as spectroscopic models for related tethered species. The ^{31}P NMR data (Table 1) for the free ligand PPM (singlets at −3.7 and −20.3 ppm) are the same as those reported in the literature [20]. Attachment of the linker *R* to form *R*-PPM (**1**), Eq. (2), results in a characteristic shift in the ^{31}P NMR spectra to −8.2 and −22.3 ppm, which is the same as observed by Pugin and Müller [5]. Addition of $[Rh(COD)_2]^+BF_4^-$ (**4**) to *R*-PPM (**1**) produces the expected but previously unreported *R*-PPM-Rh-COD (**10**) species (Scheme 2). Numerous related X-PPM-Rh-COD species have been produced by the displacement of a COD ligand from $[Rh(COD)_2]^+A^-$ (A^- is a counter anion such as BF_4^-

[1] During most of the reaction, small amounts of COD, $CODH_2$ (cyclooctene), and $CODH_4$ (cyclooctane) were also observed by GC originating from the Rh complex; the major product was $CODH_2$. After the MAC substrate was consumed, $CODH_4$ became the exclusive product.

Table 1
^{31}P NMR and ν(CO) IR data for the complexes[a]

Complex	$^{\alpha}$P	$^{\beta}$P	J_{Rh-P}	J_{Rh-P}	J_{P-P}	ν(CO) IR
PPM[b]	−3.7	−20.3				
PPM-Rh-COD (**9**)[b]	42.4	32.5	113	110	37	
R-PPM (**1**)[b]	−8.2	−22.3				
R-PPM-O_2 (**15**)[b]	32.4	31.6				
R-PPM-Rh-COD (**10**)[b]	44.2	16.8	146	140	38	
R-PPM-Rh(MeOH)$_2$ (**16**)[c]	69.7	46.0	196	196	64	
R-PPM-Rh-MeOH-CO (**20**)[c]	35.7	24.4	315	314	127	1984(s)[d]
R-PPM-Rh-MAC (**19**)[c]	50.7	22.2	152	103	19	
R-PPM-Rh-MAC (**19**)[e]	40.5	32.4	115	112	20	
R-PPM-Rh-MAC (**19**)[f]	46	33				
R-PPM-Rh-MAC-CO (**21**)[c]	54.3	47.4	137	137	125	1970(s)[d]
SiO_2-*R*-PPM (**2**)[f]	−7	−23				
SiO_2-*R*-PPM-O_2 (**11**)[f]	35	35				
SiO_2-*R*-PPM-Rh-COD (**3**)[f]	43	15				
SiO_2-*R*-PPM-Rh-MeOH-CO (**24**)[f]	35	25				1990(s)[g]
SiO_2-*R*-PPM-Rh-MAC (**23**)[f]	40	28				
SiO_2-*R*-PPM-Rh-MAC-CO (**25**)						1974(s)[g]
Pd-SiO_2-*R*-PPM (**12**)[f]	−7	−21				
Pd-SiO_2-*R*-PPM-O_2 (**13**)[f]	38	38				
Pd-SiO_2-*R*-PPM-Rh-COD (**6**)[f]	45	15				
Pd-SiO_2-*R*-PPM-Rh-MeOH-CO (**27**)[f]	35	25				1990(s)[g]
Pd-SiO_2-*R*-PPM-Rh-MAC-CO (**28**)						1974(s)[g]

[a] Chemical shifts (in ppm) are referenced to an external standard of 85% H_3PO_4 and *J* couplings are given in Hertz. ν(CO) values are given in cm^{-1}.
[b] ^{31}P NMR measured in $CDCl_3$.
[c] ^{31}P NMR measured in MeOH-d_4.
[d] Solution IR measured in CH_2Cl_2.
[e] ^{31}P NMR measured in 85% $CDCl_3$–15% MeOH-d_4.
[f] Solid-state (CPMAS) ^{31}P NMR.
[g] DRIFT.

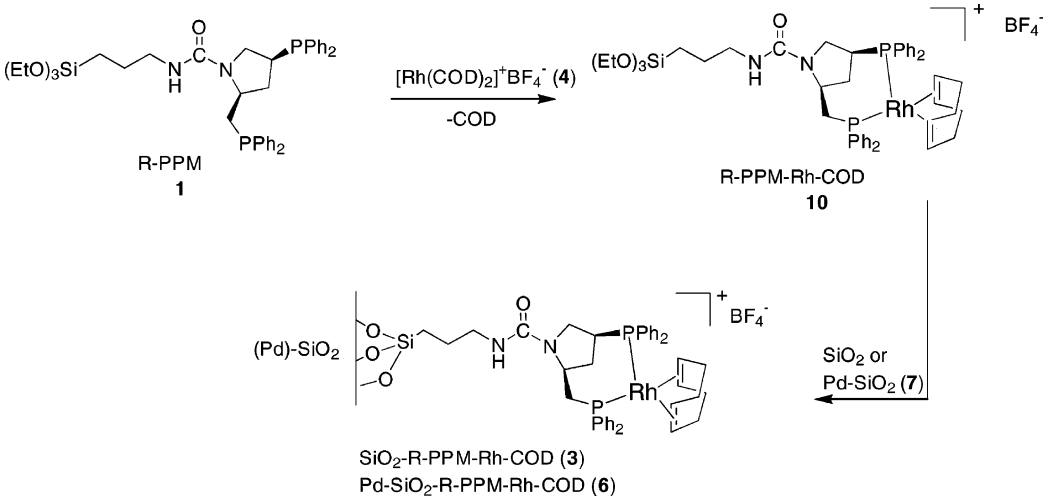

Scheme 2. Preparation of the tethered catalysts SiO_2-*R*-PPM-Rh-COD (**3**A) and Pd-SiO_2-*R*-PPM-Rh-COD (**6**A) using Method A.

or ClO_4^-) with X-PPM, where X-PPM is a PPM derivative with various X groups on the pyrrolidine nitrogen such as H, CO_2(*t*-Bu), and CO(*t*-Bu) [20–23]. The resultant *R*-PPM-Rh-COD (**10**) shows ^{31}P NMR signals that are consistent with those of other known X-PPM-Rh-COD complexes: *R*-PPM-Rh-COD (**10**) ([*R*-PPM-Rh-COD]$^+BF_4^-$) exhibits a doublet of doublets at 44.2 and 16.8 ppm with $J_{Rh-P} = 146$ and 140 Hz and $J_{P-P} = 38$ Hz; [P-PPM-Rh-COD]$^+ClO_4^-$ (**14**), in which P-PPM is an –CO(*t*-Bu) derivative of PPM, has a doublet of doublets at 43.1 and 12.1 ppm with $J_{Rh-P} = 146$ and 139 Hz and $J_{P-P} = 37$ Hz [20]; and [B-PPM-Rh-COD]$^+ClO_4^-$ (**5**), in which B-PPM is a –CO_2(*t*-Bu) derivative of PPM, exhibits a doublet of doublets at 41.6 and 12.6 ppm with $J_{Rh-P} = 145$ and 140 Hz and $J_{P-P} = 37$ Hz [20]. Note that the ^{31}P splitting pattern, consisting of two doublets of doublets resulting from coupling of the phosphines to each other as well as to the spin 1/2 rhodium establishes the complexation of PPM to rhodium in the compound. In addition, the P–P coupling constants (38 Hz) and the Rh–P coupling constant (∼140 Hz) are consistent with those seen in other X-PPM-Rh-COD complexes [20].

While PPM appears to be air stable, *R*-PPM (**1**) easily forms the phosphine oxide, *R*-PPM-O_2 (**15**) in air, Eq. (3).

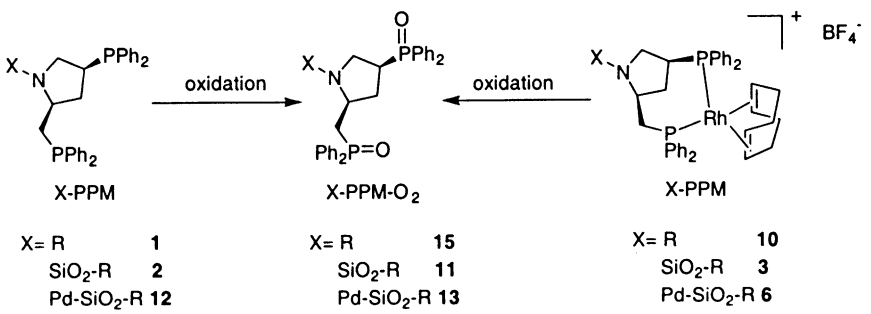

(3)

This occurs if a solution of *R*-PPM (**1**) is exposed to air for a few days at room temperature or overnight at elevated temperature (110 °C). The rhodium complex *R*-PPM-Rh-COD (**10**) is even more air sensitive, oxidizing completely overnight in solution at room temperature. The oxidation of either compound occurs within 5 min when reacted with hydrogen peroxide, H_2O_2 (30 wt.%). Oxidation of **1** or **10** by either method gives *R*-PPM-O_2 (**15**), as indicated by the ^{31}P NMR spectrum which contains singlets at 32.4 and 31.6 ppm.

3.1.2. Characterization of *R*-PPM and *(R-PPM)Rh(COD)*$^+$ species tethered on SiO_2

When *R*-PPM (**1**) is tethered to silica by refluxing in toluene with SiO_2 for 16 h, the identity of the resulting product SiO_2-*R*-PPM (**2**) was established by the similarity of its ^{31}P CPMAS NMR spectrum (Fig. 1a) to that of *R*-PPM (**1**) in solution. The solid SiO_2-*R*-PPM (**2**) shows ^{31}P NMR signals at −7 and −23 ppm; these are nearly identical to those of *R*-PPM (**1**) in solution at −8.2 and −22.3 ppm. This similarity also suggests that the tethering process does not change the environment of the *R*-PPM phosphine ligand; that is, the phosphines on the *R*-PPM ligand do not coordinate to acidic sites on the SiO_2 surface.

SiO_2-*R*-PPM (**2**) oxidizes in air to SiO_2-*R*-PPM-O_2 (**11**) slowly over a few days, Eq. (3). The oxidation of **2** with H_2O_2 (30 wt.%) in acetone at room temperature occurs completely within 5 min. The ^{31}P CPMAS spectrum of SiO_2-*R*-PPM-O_2 (**11**) consists of a broad absorption at 35 ppm (Fig. 2), which compares with two bands at 32.4 and 31.6 ppm for *R*-PPM-O_2 (**15**) in $CDCl_3$.

The tethered catalyst, SiO_2-*R*-PPM-Rh-COD (**3**), can be produced by two methodologies and is easily characterized by solid-state ^{31}P CPMAS NMR spectroscopy (Fig. 1b and c). Method A involves tethering the preformed complex *R*-PPM-Rh-COD (**10**) to the SiO_2 (Scheme 2). In Method B, the rhodium is introduced after the phosphine has been tethered to silica gel (Scheme 1). The differences in product **3** prepared by these two methods are negligible, as determined by their ^{31}P CPMAS spectra and catalytic activities (see Section 3.2.2.2.). The ^{31}P NMR spectrum of **3**, prepared by both methods, shows that the complex on the surface retains the same structure as in solution. This

is evidenced by chemical shifts of 43 and 15 ppm for **3** as compared to 44.2 and 16.8 ppm for **10** in solution.

In Method A, the rhodium:phosphine ligand ratio is fixed at 1:1 as required by the composition of the reacting *R*-PPM-Rh-COD (**10**) complex. This is reflected in the ^{31}P CPMAS spectrum, which shows signals for only SiO_2-*R*-PPM-Rh-COD (**3**), 43 and 15 ppm. In Method B, various rhodium:phophine ratios can be used depending on the amount of $[Rh(COD)_2]^+BF_4^-$ (**4**) that is added to the phosphine tethered on the surface (**2**). When an excess of phosphine is present on the surface, not only is the rhodium complex, SiO_2-*R*-PPM-Rh-COD (**3**) detected by its ^{31}P NMR signals at 43 and 15 ppm, but excess ligand, SiO_2-*R*-PPM (**2**), is also present as indicated by ^{31}P NMR signals at −7 and −23 ppm (Fig. 3). If a 1:1 ratio of rhodium to ppm is used, the ^{31}P NMR spectrum shows the presence of only the rhodium complex **3**; the absence of signals at −7 and −23 ppm indicates that all of the diphosphine ligand is coordinated. When the rhodium:phosphine ligand ratio is 2:1, the ^{31}P NMR spectrum shows the main species on the surface to be SiO_2-*R*-PPM-Rh-COD (**3**), but an unidentified minor complex, ∼15% of the sample, exhibits a band at 26 ppm (Fig. 3d).

It should be noted that for all rhodium–phosphine complexes on SiO_2 reported in this paper, the NMR signal from SiO_2-*R*-PPM-O_2 (**11**) at 35 ppm is either evident in the spectra of freshly prepared samples or grows in over time. The SiO_2-*R*-PPM-Rh-COD (**3**) is moderately to strongly air-sensitive both in the solid state and in solution. This air-sensitivity is evidenced by a decrease in intensity of ^{31}P signals of this complex, an increase in intensity of the phosphine oxide signal (35 ppm), and the appearance of a dark precipitate when **3** is exposed to air. For example, the downfield peak of the spectrum of Fig. 3b consists of two superimposed resonances representing one of the ^{31}P nuclei in **3** (at 45 ppm) and oxide **11** (at 35 ppm). Note that the ^{31}P nuclei in SiO_2-*R*-PPM-O_2 exhibit large chemical shift anisotropies, which is evidenced by the presence of spinning sidebands in the spectra taken with a lower sample spinning rate (see Fig. 2). The identity of the resonance at 35 ppm in Fig. 3b was verified by measuring the same spectrum at a lower sample spinning rate (not shown), which revealed the presence of similar spinning sidebands associated with this resonance. Solid-state ^{31}P NMR studies indicate

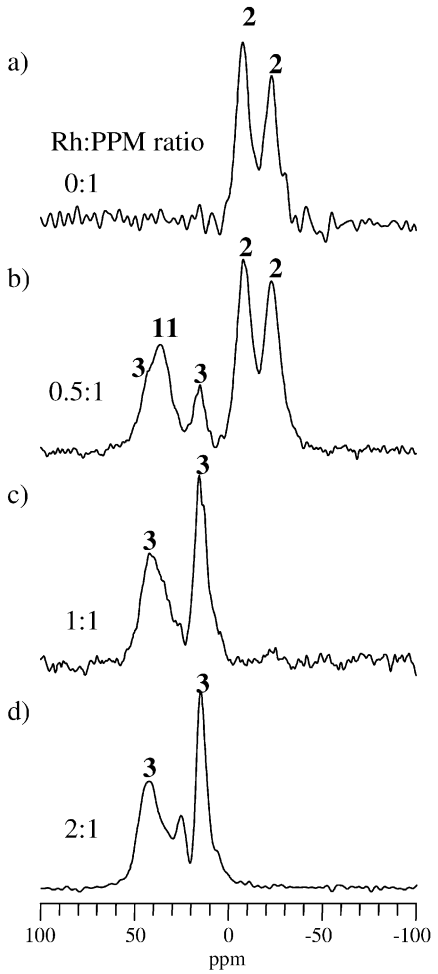

Fig. 3. ^{31}P CPMAS NMR spectra of SiO_2-*R*-PPM (**2**) (a) and its rhodium complex SiO_2-*R*-PPM-Rh-COD (**3**) obtained by Method B (b–d).

that relatively small amounts of oxygen infiltrate the rotor, such that SiO_2-*R*-PPM-Rh-COD (**3**) oxidizes to SiO_2-*R*-PPM-O_2 (**11**) at a rate of approximately 1% per hour. The air sensitivity of SiO_2-*R*-PPM-Rh-COD (**3**) raises the possibility that **3** actually consists of rhodium coordinated to SiO_2-*R*-PPM-O_2 (**11**). This, however, does not occur since the reaction of H_2O_2 with SiO_2-*R*-PPM-Rh-COD (**3**) in acetone at room temperature for 5 min gives a ^{31}P CPMAS spectrum that is identical to that of SiO_2-*R*-PPM-O_2 (**11**), which indicates that the rhodium is released from the phosphine ligand during oxidation. Indeed, when $[Rh(COD)_2]^+BF_4^-$ (**4**) is added to SiO_2-*R*-PPM-O_2

(**11**), there is no shift in the ^{31}P NMR signals for **11**, indicating that there are no interactions between SiO_2-*R*-PPM-O_2 (**11**) and rhodium. More experimental evidence for this lack of interaction is presented in Section 3.2.2.5.

3.1.3. Characterization of R-PPM and (R-PPM)Rh(COD)$^+$ species tethered on Pd-SiO_2 (7)

The Pd-SiO_2-*R*-PPM-Rh-COD (**6**) catalyst was prepared by the same two methods used in the preparation of SiO_2-*R*-PPM-Rh-COD (**3**). Method A tethers the preformed *R*-PPM-Rh-COD (**10**) complex to Pd-SiO_2 (**7**). Method B is a sequential route where the phosphine, *R*-PPM (**1**), is tethered to Pd-SiO_2 (**7**) before rhodium is complexed. In Method B, the ^{31}P CPMAS spectrum of Pd-SiO_2-*R*-PPM (**12**) (Fig. 1d), prior to the addition of rhodium, exhibits peaks at −7 and −21 ppm, which are very similar to those of SiO_2-*R*-PPM (**2**) (−7 and −23 ppm) and *R*-PPM (**1**) (−8.2 and −22.3 ppm) [24]. Addition of one equivalent of $[Rh(COD)_2]^+BF_4^-$ (**4**) to **12** produces Pd-SiO_2-*R*-PPM-Rh-COD (**6**B). The ^{31}P NMR spectrum of this product is shown in Fig. 1f. The corresponding spectrum of Pd-SiO_2-*R*-PPM-Rh-COD prepared using Method A (**6**A) is shown in Fig. 1e. As expected, the spectra of Fig. 1b, c and e are very similar and consistent with either the presence of **3** or **6**. The spectrum of Fig. 1f shows the effect of oxidation, as the resonances of **11** centered at 35 ppm overwhelm the weaker lines at 45 and 15 ppm. More detailed ^{31}P NMR studies revealed that **6** is as air sensitive as **3**, i.e. the oxidation rates in the NMR rotor are approximately 1% per hour. Again, the oxidation of either **12** or **6** with H_2O_2 produces Pd-SiO_2-*R*-PPM-O_2 (**13**), Eq. (3), which exhibits a broad signal at around 35 ppm. Furthermore, the addition of Rh complex **4** to **13** causes no change in the ^{31}P NMR spectrum, confirming that the phosphine oxide of PPM does not coordinate to rhodium.

3.2. Characterization of catalysts after use in the hydrogenation of MAC

3.2.1. Characterization of the catalytic species in solution

The generally accepted catalytic cycle for enantioselective hydrogenation of olefins by cationic rhodium complexes with chelating ligands [20,21,25–31] is shown in the lower part of Scheme 3. In the first step, Eq. (a), open coordination sites on the rhodium are generated by the hydrogenation of the COD ligand (see footnote 1). The resulting methanol-solvated species then coordinates the MAC substrate in a bidentate fashion, Eq. (b). Oxidative addition of hydrogen, Eq. (c), is followed by rapid sequential hydrogen transfer, Eqs. (d) and (e). The hydrogenated product $MACH_2$ is a poor substrate for binding to the rhodium and is displaced by solvent to regenerate the starting complex in the catalytic cycle.

The ^{31}P NMR spectra of PPM, *R*-PPM (**1**), and *R*-PPM-Rh-COD (**10**) were discussed in Section 3.1.1. It is known that the Rh in X-PPM-Rh-COD complexes binds to coordinating solvents after COD is hydrogenated [20,22,25–28,32]. *R*-PPM-Rh-COD (**10**) also exhibits this behavior. In methanol at room temperature under 1 atm of hydrogen, COD in **10** is hydrogenated to produce the di-methanol complex *R*-PPM-Rh$(MeOH)_2$ (**16**), whose ^{31}P NMR spectrum is consistent with other X-PPM-Rh$(MeOH)_2$ species. In particular, *R*-PPM-Rh$(MeOH)_2$ (**16**) exhibits a doublet of doublets at 69.7 and 46.0 ppm with J_{Rh-P} = 196 and 196 Hz and J_{P-P} = 64 Hz, while the known [20] $[$P-PPM-Rh$(MeOH)_2]^+ClO_4^-$ (**17**) exhibits a doublet of doublets at 69.6 and 42.5 ppm with J_{Rh-P} = 201 and 197 Hz and J_{P-P} = 65 Hz, and $[$B-PPM-Rh$(MeOH)_2]^+ClO_4^-$ (**18**) exhibits a doublet of doublets at 68.0 and 42.2 ppm with J_{Rh-P} = 200 and 197 Hz and J_{P-P} = 66 Hz [20]. When five equivalents of MAC are added to a methanol solution of *R*-PPM-Rh$(MeOH)_2$ (**16**) the ^{31}P NMR spectrum exhibits a doublet of doublets at 50.7 and 22.2 ppm with J_{Rh-P} = 152 and 103 Hz and J_{P-P} = 19 Hz, which is assigned to *R*-PPM-Rh-MAC (**19**). The two phosphorus signals move closer to each other when the MeOH-d_4 solvent is partially replaced with $CDCl_3$. At 85% $CDCl_3$ and 15% MeOH-d_4, the ^{31}P NMR signals are at 40.5 and 32.4 ppm. Because of this dramatic solvent dependency, solid-state NMR spectroscopy of (**19**) was run and yielded two ^{31}P peaks at 46 and 33 ppm (spectrum not shown).

In order to gain more information about the species present in the catalytic cycle (Scheme 3), we reacted likely intermediates with CO to give more air-stable complexes. Such reactions of rhodium complexes of PPM (or its derivatives) with CO have

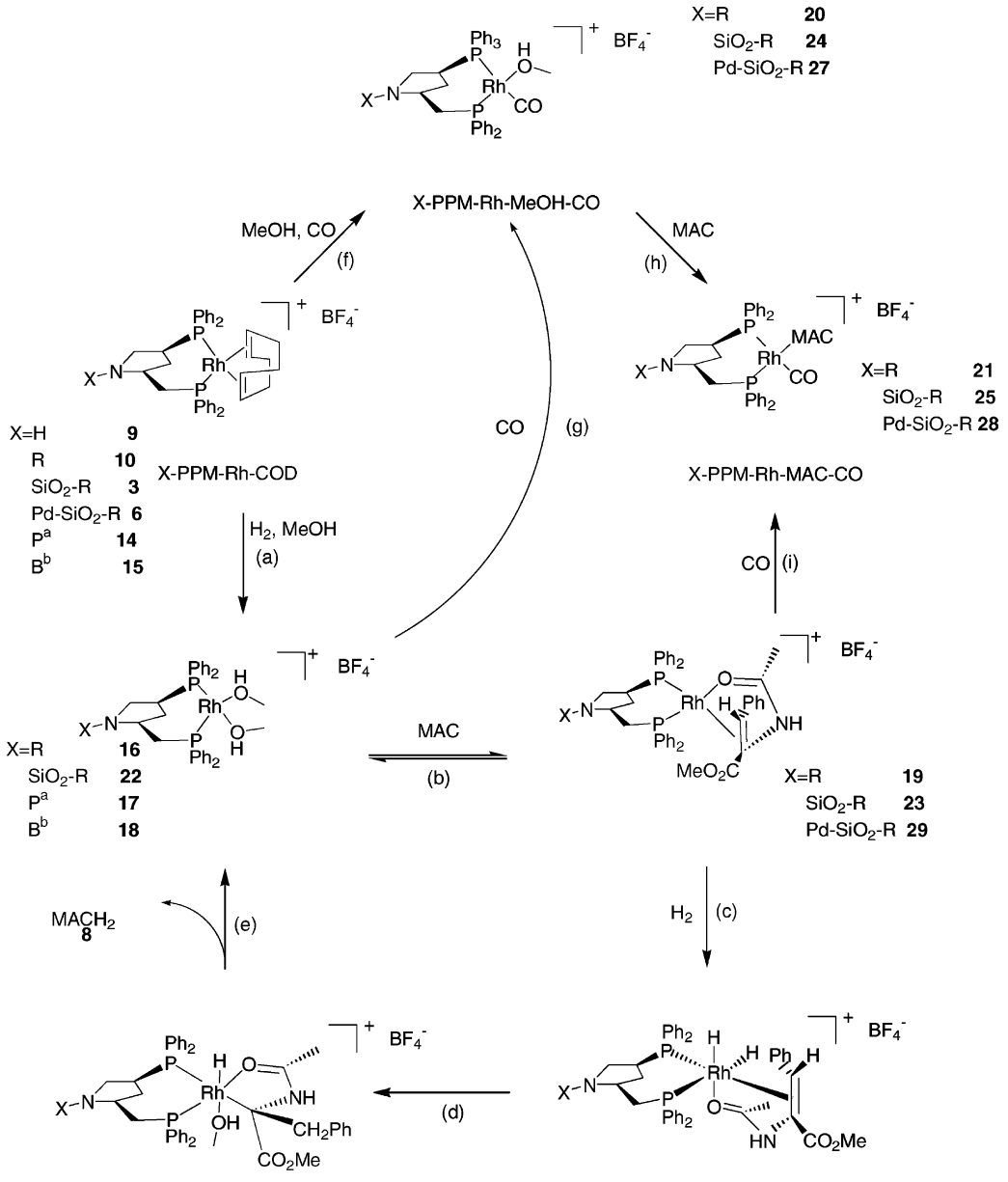

[a]P= -CO(t-Bu) see ref [20]. [b]B= -CO_2(t-Bu), see ref [20].

Scheme 3. Catalytic cycle for the hydrogenation of MAC using PPM-Rh and reactions of intermediates with CO.

not been previously reported; however, CO reactions with other cationic rhodium–phosphine complexes are well-known [32–34]. When CO is bubbled through a MeOH solution of *R*-PPM-Rh-COD (**10**) at room temperature for 10 min (Scheme 3, Eq. (f)), *R*-PPM-Rh-MeOH-CO (**20**) is produced. During the reaction, the color of the solution bleaches from bright yellow to pale yellow–green. The ^{31}P NMR

spectrum of this solution exhibits a doublet of doublets at 35.7 and 24.4 ppm, $J_{Rh-P} = 315$ and 314 Hz and $J_{P-P} = 127$ Hz. In the IR spectrum, a ν(CO) band appears at 1984 cm^{-1}. This ν(CO) band corresponds well with other cationic rhodium(I) carbonyl species such as $L_2Rh(solvent)(CO)^+$, where L = PPh_3, PPh_2Me and solvent = DMA, DMF; all of these complexes show ν(CO) bands [32] in the same range (1971–2000 cm^{-1}) as that assigned to *R*-PPM-Rh-MeOH-CO (**20**). Complex **20** is also formed when CO is bubbled through a MeOH solution of *R*-PPM-Rh$(MeOH)_2$ (**16**) (Scheme 3, Eq. (g)), as established by its ^{31}P NMR and ν(CO) IR spectra.

The reaction of *R*-PPM-Rh-MeOH-CO (**20**) in MeOH with 5 eq. of MAC gives *R*-PPM-Rh-MAC-CO (**21**) (Scheme 3, Eq. (h)). It is also produced (Scheme 3, Eq. (i)) when CO is bubbled for 10 min through a methanol solution of *R*-PPM-Rh-MAC (**19**) at room temperature. Both methods yield a product identical by IR (ν(CO) 1970(s) cm^{-1}) and ^{31}P NMR (doublets of doublets at 54.3 and 47.4 ppm, $J_{Rh-P} = 137$ and 137 Hz and $J_{P-P} = 125$ Hz).

The B-PPM-Rh-COD complex **15** is reported to catalyze the hydrogenation of MAC (Eq. (1)) with a TOF of 14.3 min^{-1} and an enantioselectivity of 94.5% ee [5]. Our measured rates and enantioselectivities of *R*-PPM-Rh-COD (**10**) in solution are slightly lower, TOF 5.01 min^{-1} and 93.5% ee. The enantioselective hydrogenation of MAC using *R*-PPM-Rh-COD (**10**) and the identification of possible intermediates **16** and **19** described above suggests that **10** catalyzes the hydrogenation of MAC by the mechanism (Scheme 3) indicated for related reactions [20,21,25–31]. Neither of the CO adducts, *R*-PPM-Rh-MAC-CO (**21**) nor *R*-PPM-Rh-MeOH-CO (**20**), exhibit any activity for the hydrogenation of MAC.

3.2.2. *Characterization of the catalytic species tethered on SiO_2*

3.2.2.1. CO derivatives. Unfortunately, the catalytic species present during and after hydrogenation are too air sensitive to be observed by the solid-state ^{31}P NMR techniques used in this study. Although samples from the reactions are handled under argon and loaded into the NMR rotor in a glove bag under nitrogen, the rotor itself is not completely air tight under NMR acquisition conditions. All samples obtained from the hydrogenation reactions gave poor spectra. Reduced intensities of all signals and an increase in intensity of a peak at 35 ppm corresponding to SiO_2-*R*-PPM-O_2 (**11**) are observed.

Attempts to produce a characterizable SiO_2-*R*-PPM-Rh$(MeOH)_2$ (**22**) species by hydrogenating off COD in the absence of MAC resulted in poor ^{31}P NMR spectra whose only discernable signal represented the phosphine oxide **11**. If the di-MeOH species (**22**) is not separated from the reaction mixture but instead 5 eq. of MAC are added under an atmosphere of argon, SiO_2-*R*-PPM-Rh-MAC (**23**) was detected by its solid-state ^{31}P signals at 40 and 28 ppm which compare closely to the converging signals of *R*-PPM-Rh-MAC (**19**) in 85% $CDCl_3$/15% MeOH-d_4 solution (40.5 and 32.4 ppm) as well as the signals of solid **19** (46 and 33 ppm), see Section 3.2.1.

Reactions of the various rhodium phosphine complexes tethered to SiO_2 with CO give species that are sufficiently air stable to give observable solid-state ^{31}P NMR and DRIFT spectra (not shown). As observed for *R*-PPM-Rh-COD (**10**), SiO_2-*R*-PPM-Rh-COD (**3**) in MeOH reacts with bubbling CO for 15 min. After solvent removal under vacuum, the resulting solid gave DRIFT (ν(CO) 1990(s) cm^{-1}) and ^{31}P CPMAS NMR spectra (35 and 25 ppm) that are very similar to those of the solution species *R*-PPM-Rh-MeOH-CO (**20**) (IR: ν(CO) 1984(s) cm^{-1}; ^{31}P NMR in solution of MeOH-d_4: 35.7 and 24.4 ppm). This suggests that the species on the surface is SiO_2-*R*-PPM-Rh-MeOH-CO (**24**).

SiO_2-*R*-PPM-Rh-MAC-CO (**25**) is obtained by two independent methods. It is the product when 5 eq. of MAC are added to SiO_2-*R*-PPM-Rh-MeOH-CO (**24**) in a methanol solution at room temperature (Scheme 3, Eq. (h)). Or, it is formed in the reaction of SiO_2-*R*-PPM-Rh-MAC (**23**) with CO in methanol at room temperature for 15 min (Scheme 3, Eq. (i)). Both methods yield the same product as established by DRIFT spectroscopy. Assignment of the structure to product **25** is based on the similarity of the DRIFT (ν(CO) 1974(s) cm^{-1}) spectrum of **25** to that (IR: ν(CO) 1970(s) cm^{-1}) of the *R*-PPM-Rh-MAC-CO (**21**) complex in solution.

Reaction of CO with SiO_2-*R*-PPM-Rh-COD (**3**) during or after MAC hydrogenation in methanol results in DRIFT bands readily ascribable to either SiO_2-*R*-PPM-Rh-MeOH-CO (**24**) or SiO_2-*R*-PPM-

Rh-MAC-CO (**25**) depending on when the CO is introduced. If the hydrogenation of MAC is stopped before MAC is completely hydrogenated and the hydrogen atmosphere is replaced with CO, the resulting rhodium-CO species exhibits a ν(CO) band at 1974 cm^{-1} consistent with SiO_2-*R*-PPM-Rh-MAC-CO (**25**). The absence of additional ν(CO) bands indicates that Rh(0) and Rh(I) on SiO_2 are not present since their CO adducts would give bands at 2095 and 2027 cm^{-1} or 2040–2066 cm^{-1} [35–38]. Replacing the hydrogen atmosphere with CO after the complete hydrogenation of MAC gives SiO_2-*R*-PPM-Rh-MeOH-CO (**24**) as indicated by the ν(CO) band at 1990(s) cm^{-1}. The ^{31}P CPMAS NMR spectrum with absorptions at 35 and 25 ppm supports this assignment. This is a reasonable product as $MACH_2$ is a very weak ligand and only methanol remains for coordination. The lack of additional DRIFT ν(CO) bands conclusively shows that the PPM-Rh unit remains intact.

Thus, reactions of CO with the tethered catalyst at various stages of the hydrogenation indicate that the reaction mechanism on the surface mimics that proposed for the analogous reaction in solution (Scheme 3, Eqs. (a–e)). These studies also show that the rhodium remains coordinated to the phosphorus throughout the reaction since no DRIFT ν(CO) bands other than those assignable to SiO_2-*R*-PPM-Rh-MeOH-CO (**24**) or SiO_2-*R*-PPM-Rh-MAC-CO (**25**) are observed. Rate data, enantioselectivities, and mercury poisoning experiments, presented below, further support these conclusions.

3.2.2.2. Activity and enantioselectivity studies of the hydrogenation of MAC. Pugin and Müller [5] reports that SiO_2-*R*-PPM-Rh-COD (**3**) prepared by Method B (Scheme 1) gives rates (TOF) varying from 6.25 to 12.5 min^{-1} with ee values ranging from 89.8 to 94.5% depending on the catalyst batch. Our catalysts prepared by Method B give an average TOF value of 11.2 min^{-1} and an average ee of 91.1% (entry 5, Table 2). This indicates that our catalysts are the same as Pugin's. In addition, we observe that the catalyst formed by Method A (entry 4) gives a similar average rate (TOF = 13.8 min^{-1}) and enantioselectivity (ee = 93.7%). The comparable rates and enantioselectivities reinforce the previous spectroscopic evidence that the catalysts prepared by either Method A or Method B are the same.

3.2.2.3. Mercury poisoning experiments. In order to exclude the possibility that the hydrogenation of MAC over SiO_2-*R*-PPM-Rh-COD (**3**) occurs on metallic rhodium particles deposited from the tethered rhodium complex, studies of the effect of mercury metal were undertaken. It is known that mercury poisons nano-metal catalysts ([39] and references therein) and supported metal catalysts [40] that catalyze olefin and arene hydrogenation reactions. However, mercury does not affect the activities of homogeneous metal catalysts ([39] and references therein). Thus, the addition of mercury is a standard method for determining whether a reaction is catalyzed by a metal or a metal complex. We observe that mercury has no effect on the rate or enantioselectivity (entry 6, Table 2) of the hydrogenation of MAC catalyzed by SiO_2-*R*-PPM-Rh-COD (**3**). Thus, the catalytically active species in SiO_2-*R*-PPM-Rh-COD (**3**) is the 'homogeneous' *R*-PPM-Rh-COD (**10**) metal complex bound to the silica surface and not rhodium metal.

*3.2.2.4. Catalytic activity of $[Rh(COD)_2]^+BF_4^-$/SiO_2 (**26**).* In order to explore the possibility that rhodium metal without phosphine ligands is able to catalyze the hydrogenation of MAC, $[Rh(COD)_2]^+BF_4^-$ (**4**) was adsorbed on SiO_2, by stirring $[Rh(COD)_2]^+BF_4^-$ (**4**) with SiO_2 for 5 min in the absence of any phosphine. The resulting solid exhibits (entry 7, Table 2) very low activity (TOF = 0.0600 min^{-1}) for the hydrogenation of MAC under the usual reaction conditions (25 °C, 1 atm H_2, MeOH solvent). The rate of MAC hydrogenation with $[Rh(COD)_2]^+BF_4^-/SiO_2$ (**26**) is at least two-orders of magnitude slower than the same hydrogenation with SiO_2-*R*-PPM-Rh-COD (**3**), and as expected, $[Rh(COD)_2]^+BF_4^-/SiO_2$ (**26**) produces racemic $MACH_2$ (**8**). Moreover, mercury quenches the hydrogenation reaction completely. This latter experiment also indicates that the active hydrogenation species must be metallic rhodium resulting from the reduction of $[Rh(COD)_2]^+BF_4^-$ (**4**). This is consistent with our observations in studies of $[Rh(COD)_2]^+BF_4^-$ (**4**) [18] in other hydrogenation reactions.

*3.2.2.5. Effect of air on the catalytic activity of SiO_2-R-PPM-Rh-COD (**3**).* When SiO_2-*R*-PPM-Rh-COD (**3**) prepared by Method A is partially oxidized by exposure to air for 5 days, its activity

Table 2
Hydrogenation of MAC[a]

Entry	Species	Rate[b] (TOF[c], min^{-1})	ee[d] (%)
1	B-PPM-Rh-COD (lit)[e] (**5**)	14.3[e]	94.5[e]
2	*R*-PPM-Rh-COD (**10**)	5.01	93.5
3	SiO_2-*R*-PPM-Rh-COD (lit)[e] (**3**)	6.25–12.5[e]	89.8–94.5[e]
4	SiO_2-*R*-PPM-Rh-COD(preformed)[f] (**3**A)	13.8	93.7
5	SiO_2-*R*-PPM-Rh-COD(sequential)[g] (**3**B)	11.2	91.1
6	SiO_2-*R*-PPM-Rh-COD (**3**) plus Hg[h]	12.0	92.5
7	SiO_2 plus $[Rh(COD)_2]^+BF_4^-$[i] (**26**)	0.0600	Racemic
8	SiO_2 plus $[Rh(COD)_2]^+BF_4^-$[i] (**26**) plus Hg[h]	0.00	
9	Oxidized SiO_2-*R*-PPM-Rh-COD[j]	1.02[k]	90.5[l]
10	Oxidized SiO_2-*R*-PPM-Rh-COD[m]	0.00	
11	SiO_2-*R*-PPM-O_2 (**11**) plus $[Rh(COD)2]^+BF_4^-$[i] (**4**)	0.0135	Racemic
12	Used SiO_2-*R*-PPM-Rh-COD[f] (**3**A)	7.51, 4.04[n]	93.0, 94.0[n]
13	Pd-SiO_2-*R*-PPM-Rh-COD (preformed)[f] (**6**A)	5.69	90.6
14	Pd-SiO_2-*R*-PPM-Rh-COD (sequential)[g] (**6**B)	11.8[e]	88.3
15	Pd-SiO_2-*R*-PPM-Rh-COD (preformed)[f] (**6**A) plus Hg[h]	6.11	92.0
16	Pd-SiO_2-*R*-PPM-Rh-COD (sequential)[g] (**6**B) plus Hg[h]	10.4	85.0
17	Used Pd-SiO_2-*R*-PPM-Rh-COD (preformed)[f] (**6**A)	5.02, 4.01[n], 5.04[o]	89.3, 92.0[n], 92.0[o]
18	Pd-SiO_2 (**7**)	7.06[p]	Racemic
19	Pd-SiO_2 (**7**) plus $[Rh(COD)_2]^+BF_4^-$[i] (**4**)	12.5	Racemic
20	Oxidized Pd-SiO_2-*R*-PPM-Rh-COD[j]	3.02	16.0
21	Pd-SiO_2-*R*-PPM-O_2 (**13**) plus $[Rh(COD)_2]^+BF_4^-$[i] (**4**)	11.7	Racemic
22	Pd-SiO_2 (**7**) plus $[Rh(COD)_2]^+BF_4^-$[i] (**4**) plus Hg[h]	0.00	
23	1% Pd-SiO_2-*R*-PPM-Rh-COD (sequential)[g] (**6**B)	10.2	86.8

[a] See Eq. (1). Typical reaction conditions: 14 mg of catalyst (3.75 μmol Rh), 750 μmol (200 eq.) MAC, 7.5 ml MeOH, 25 °C, 1 atm H_2. Data represents the average of three or more runs; however, Hg and re-use experiments reflect data from one unique experimental run.
[b] Rate given as TOF [mol H_2/(mol Rh·min)].
[c] TOF calculated after 5 min of reaction, corresponding to the maximum TOF observed.
[d] Enantiomeric excess (ee) determined by GC after complete hydrogenation of MAC, Chirasil-Val column (50 m × 250 μm).
[e] Literature reference [5].
[f] The catalyst was prepared using Method A.
[g] The catalyst was prepared using Method B.
[h] 0.10 ml of Hg added with MAC.
[i] Formed by stirring $[Rh(COD)_2]^+BF_4^-$ and SiO_2 for 5 min at room temperature in MeOH.
[j] Oxidized by exposure to air for 3–5 days.
[k] Activity ceases within 0.5 h of reaction, before complete MAC hydrogenation.
[l] ee for partially reacted substrate.
[m] Oxidized by addition of H_2O_2 to an acetone slurry of the catalyst prior to reaction.
[n] Second use.
[o] Third use.
[p] See footnote 2.

(entry 9, Table 2) for the hydrogenation of MAC is very low. Interestingly, the remaining activity, TOF = 1.02 min^{-1}, is enantioselective (ee = 90.5%). Presumably a small amount (∼2%) of the complex remains unoxidized and is responsible for the activity. However, when SiO_2-*R*-PPM-Rh-COD (**3**) prepared by Method A is oxidized by reaction with a few drops of H_2O_2 in acetone at room temperature for 15 min, the catalyst is completely inactive (entry 10). The addition of $[Rh(COD)_2]^+BF_4^-$ (**4**) in methanol to SiO_2-*R*-PPM-O_2 (**11**) produces a catalyst (entry 11) with very low activity (TOF = 0.0135), which exhibits no enantioselectivity. This result supports the ^{31}P NMR studies (see Section 3.1.2), which showed that rhodium does not bind to SiO_2-*R*-PPM-O_2 (**11**). The poor activity and lack of enantioselectivity of this catalyst (entry 11) is the same as that for $[Rh(COD)_2]^+BF_4^-/SiO_2$ (**26**) (entry 7).

Table 3
Effect of Rh:PPM ratio on the activity and enantioselectivity of SiO_2-*R*-PPM-Rh-COD (**3**B), prepared by Method B, in the hydrogenation of MAC[a]

Rh:PPM	Rate (TOF, min^{-1})	ee[b] (%)
0.5:1	8.83[c]	90.5
Plus Hg	9.04[c]	90.0
1:1	11.2[c]	91.5
Plus Hg	11.0[c]	92.5
2:1	12.0[d]	90.1
Plus Hg	11.0[d]	91.8
4:1	8.84[d]	92.7
Plus Hg	10.8[d]	92.4

[a] Reaction conditions are the same as those in Table 2.
[b] Enantiomeric excess determined by GC after complete hydrogenation of MAC.
[c] TOF [mol H_2/(mol Rh·min)] after the first 5 min of reaction, corresponding to the maximum TOF observed.
[d] TOF [mol H_2/(mol PPM·min)] after the first 5 min of reaction, corresponding to the maximum TOF observed.

*3.2.2.6. Effect of Rh/PPM ratio on SiO_2-R-PPM-Rh-COD (**3**) activity.* When the catalyst SiO_2-*R*-PPM-Rh-COD (**3**) is formed by reaction of the rhodium complex *R*-PPM-Rh-COD (**10**) with SiO_2 (Method A), the rhodium:phosphorus ratio is fixed at 1:1; the TOF and ee values for this catalyst (entry 4, Table 2) are 13.8 min^{-1} and 93.7% respectively. When **3** is prepared by sequential addition of $[Rh(COD)_2]^+BF_4^-$ (**4**) to SiO_2-*R*-PPM (**2**) (Method B), a 0.5:1 ratio of rhodium to PPM yields a catalyst with an activity that reflects the amount of rhodium that is in the form of **3**; its TOF and ee values are 8.83 min^{-1} and 90.5%, respectively (Table 3). With a 1:1 ratio of rhodium to PPM the activities are TOF (11.2 min^{-1}) and ee (91.5%). When a 2:1 ratio of rhodium to PPM is incorporated into **3**, the enantioselectivity is 90.1%, and if the TOF is calculated based on the total amount of rhodium in the system, the TOF is 6.00 min^{-1}. This value is low in comparison to all of the other TOF values for SiO_2-*R*-PPM-Rh-COD (**3**). If the phosphine content, instead of the rhodium content, is used to calculate the amount of **3** present, then a TOF value of 12.0 min^{-1} is obtained, which is consistent with the other TOF values. It is logical to calculate TOF this way since the phosphine is the limiting reagent in the formation of the rhodium–PPM complex and represents the maximum amount of the complex possible. For the catalyst with a 2:1 rhodium to PPM ratio, one equivalent of rhodium is not complexed and presumably deposits on the SiO_2 surface where it is a poor MAC hydrogenation catalyst (see Section 3.2.2.4.). For the catalyst with a 4:1 rhodium:PPM ratio, the enantioselectivity (ee = 92.7%) continues to be high and the rate (TOF = 8.84 min^{-1}) based on PPM content is reasonable; on the other hand, the rate (TOF = 2.21 min^{-1}) based on rhodium content is unreasonably low. Finally, for **3** prepared by Methods A or B with ratios of (Rh:PPM = 0.5:1, 1:1, 2:1, or 4:1), mercury has no effect on the rate or enantioselectivity of the reaction (Table 3). Thus, **3** containing the $[(R\text{-PPM})Rh(COD)]^+BF_4^-$ complex is the only species that catalyzes the enantioselective hydrogenation of MAC in this system.

*3.2.3. Characterization of the catalytic species tethered on Pd-SiO_2 (**7**)*

3.2.3.1. CO derivatives. The species Pd-SiO_2-*R*-PPM-Rh-MeOH-CO (**27**), obtained by stirring a methanol slurry of Pd-SiO_2-*R*-PPM-Rh-COD (**6**) under a CO atmosphere for 15 min at room temperature, gives DRIFT (ν(CO) 1990(s) cm^{-1}) and solid-state ^{31}P NMR (35 and 25 ppm) spectra that are very similar to those of SiO_2-*R*-PPM-Rh-MeOH-CO (**24**) (DRIFT (ν(CO) 1990(s) cm^{-1}) and ^{31}P NMR (35 and 25 ppm)) and *R*-PPM-Rh-MeOH-CO (**20**) (IR: (ν(CO) 1984(s) cm^{-1}) and ^{31}P NMR (35.7 and 24.4 ppm) in solution). Under the same conditions, Pd-SiO_2-*R*-PPM-Rh-MAC-CO (**28**) is produced from Pd-SiO_2-*R*-PPM-Rh-MAC (**29**) and CO (Scheme 3, Eq. (i)). The infrared spectrum (DRIFT ν(CO) 1974(s) cm^{-1}) of Pd-SiO_2-*R*-PPM-Rh-MAC-CO (**28**) is very similar to that (ν(CO) 1974(s) cm^{-1}) of SiO_2-*R*-PPM-Rh-MAC-CO (**25**) and that (ν(CO) 1970(s) cm^{-1}) of *R*-PPM-Rh-MAC-CO (**21**). Exposure of Pd-SiO_2-*R*-PPM-Rh-COD (**6**) to CO prior to MAC addition or after complete hydrogenation of MAC yields Pd-SiO_2-*R*-PPM-Rh-MeOH-CO (**27**). Exposure to CO during the reaction results in the formation of Pd-SiO_2-*R*-PPM-Rh-MAC-CO (**29**). This is the same behavior that is observed with SiO_2-*R*-PPM-Rh-COD (**3**).

3.2.3.2. Catalytic activities. The hydrogenation reactions of MAC catalyzed by Pd-SiO_2-*R*-PPM-Rh-COD (**6**A and **6**B) in which the Rh to PPM ratio is

1:1, prepared by either Method A or Method B are highly enantioselective, ee 90.6 and 88.3%, respectively (entries 13 and 14, Table 2). The sequentially prepared catalyst Pd-SiO_2-*R*-PPM-Rh-COD (**6**B), exhibits rates (TOF) of 11.8 min^{-1}. This is comparable to that of SiO_2-*R*-PPM-Rh-COD (**3**B), where the TOF is 11.2 min^{-1}. Catalyst **6**A (entry 13) shows lower rates of MAC hydrogenation (TOF = 5.69 min^{-1}) compared to that (entry 4) of SiO_2-*R*-PPM-Rh-COD (**3**A) (TOF = 13.8 min^{-1}); the reason for this lower activity is unknown. If the sequentially prepared catalyst (**6**B) contains excess rhodium, i.e. the Rh:PPM ratio is greater than 1:1, then reduced enantioselectivities are observed, see Section 4.3. For example, a catalyst prepared with a Rh:PPM ratio of 5:1 provides an ee of 22.0% after the first 5 min of reaction.

Pd-SiO_2 (**7**) by itself is a catalyst for the hydrogenation of MAC (TOF_{eff} = 7.06),[2] but the hydrogenation gives a racemic product (entry 18, Table 2). In order to determine whether rhodium adsorbed on Pd-SiO_2 (**7**) without the tethering PPM ligand would be catalytically active, $[Rh(COD)_2]^+BF_4^-$ (**4**) was adsorbed on Pd-SiO_2 (**7**) by stirring a methanol solution of $[Rh(COD)_2]^+BF_4^-$ (**4**) with Pd-SiO_2 (**7**). This system (entry 19) is highly active for the hydrogenation of MAC (TOF = 12.5 min^{-1}) but the product is completely racemic. When Pd-SiO_2-*R*-PPM-O_2 (**13**) is reacted with $[Rh(COD)_2]^+BF_4^-$ (**4**), it gives an active catalyst (TOF = 11.7 min^{-1}) but the product is racemic (entry 21). This rate is very similar to $[Rh(COD)_2]^+BF_4^-$ (**4**) on Pd-SiO_2 (**7**) (entry 19) and reaffirms the spectroscopic results (Sections 3.1.2 and 3.1.3.) that PPM-O_2 does not coordinate to Rh. Also, while mercury does not decrease the rate or enantioselectivity of Pd-SiO_2-*R*-PPM-Rh-COD (**6**), it quenches the activity of $[Rh(COD)_2]^+BF_4^-$ (**4**) on Pd-SiO_2 (**7**) (entry 22). Thus, the racemic hydrogenation activity of $[Rh(COD)_2]^+BF_4^-$ (**4**) on Pd-SiO_2 (**7**) must be attributed to metallic Rh on the silica surface. Since Rh on SiO_2 without Pd is not active (entry 7), the activation of the Rh must be due to the Pd in the system. One possibility is that hydrogen spillover from Pd reduces the $[Rh(COD)_2]^+BF_4^-$ to Rh metal. This has been shown to occur for related systems during other hydrogenation reactions [18].

The effect of Pd loading on the surface was explored briefly. A palladium loading lower than 10% was examined with some 1% w/w Pd catalysts. The 1%-Pd-SiO_2-*R*-PPM-Rh-COD (**6***B* − 1**%**) catalyst formed using Method B exhibited a rate (TOF = 10.2 min^{-1}) and enantioselectivity (ee = 86.8%) very similar to those of the analogous 10%-Pd catalyst Pd-SiO_2-*R*-PPM-Rh-COD (**6**B). The lower palladium content neither significantly raised nor lowered the MAC hydrogenation activity compared to the catalyst on 10%-Pd-SiO_2 or SiO_2. Thus from entry 23, Table 2, it can be seen that the Pd loading or even the absence of Pd had no effect on either the rates or enantioselectivities of MAC hydrogenation.

3.3. Arene hydrogenations studies

3.3.1. SiO_2-*R*-PPM-Rh-COD (*3*)

SiO_2-*R*-PPM-Rh-COD (**3**) exhibits very low, but detectable, hydrogenation activity (TOF = 0.0135 min^{-1}) for the conversion of toluene to methylcyclohexane (entry 3, Table 4). However, when the same catalyst is used for toluene hydrogenation in the presence of mercury, no activity is observed (entry 4). This result indicates that the active *arene* hydrogenation species is a heterogenized metallic rhodium species resulting from partial decomposition of SiO_2-*R*-PPM-Rh-COD (**3**). Support for this interpretation is the higher activity (TOF = 0.0604 min^{-1}) of the catalyst (entry 1) prepared by adsorbing $[Rh(COD)_2]^+BF_4^-$ onto SiO_2, **26**. The toluene hydrogenation activity of this catalyst is quenched by the addition of mercury (entry 2); this also indicates that a rhodium metal species is the active arene hydrogenation catalyst.

3.3.2. Pd-SiO_2-*R*-PPM-Rh-COD (*6*)

The catalyst Pd-SiO_2-*R*-PPM-Rh-COD (**6**) is much more active (TOF = 0.124 min^{-1}) for the hydrogenation of toluene (entry 6, Table 4) than SiO_2-*R*-PPM-Rh-COD (**3**) (TOF = 0.0135 min^{-1}) which does not contain palladium. However, the activity of Pd-SiO_2-*R*-PPM-Rh-COD (**6**) (TOF = 0.124 min^{-1}) is not much higher than that (entry 5) of simply Pd-SiO_2 (**7**) (TOF_{eff} = 0.0785 min^{-1},

[2] To facilitate comparison, the rates for Pd catalysts are reported in terms of an effective TOF, TOF_{eff}. Since these Pd-SiO_2 samples do not contain rhodium, a TOF based on rhodium content cannot be given. The TOF_{eff} value is calculated by assuming that the Pd-SiO_2 catalyst contains the standard rhodium loading (13.4 μmol/50 mg).

Table 4
Hydrogenation of toluene to methylcyclohexane[a]

Entry	Species	Rate (TOF[b], min^{-1})
1	SiO_2 plus $[Rh(COD)_2]^+BF_4^-$[c] (**26**)	0.0604
2	SiO_2 plus $[Rh(COD)_2]^+BF_4^-$[c] (**26**) plus Hg[d]	0.00
3	SiO_2-*R*-PPM-Rh-COD (**3**)	0.0135
4	SiO_2-*R*-PPM-Rh-COD (**3**) plus Hg[d]	0.00
5	Pd-SiO_2 (**7**)	0.0785[e]
6	Pd-SiO_2-*R*-PPM-Rh-COD (**6**)	0.124
7	Pd-SiO_2-*R*-PPM-Rh-COD (**6**) plus Hg[d]	0.00
8	Pd-SiO_2-*R*-PPM-Rh-COD oxidized with H_2O_2[f]	0.834
9	Pd-SiO_2 (**7**) plus $[Rh(COD)_2]^+BF_4^-$[c] (**4**)	1.65
10	Pd-SiO_2 (**7**) plus $[Rh(COD)_2]^+BF_4^-$[c] (**4**) plus Hg[d]	0.0182[g]

[a] Typical reaction conditions: 50.0 mg of catalyst (13.4 μmol Rh), 5.0 ml of toluene as both reactant and solvent, 1 atm H_2, 40 °C.
[b] TOF [mol H_2/(mol Rh·min)] after the first 5 min of reaction, corresponding to the maximum TOF observed.
[c] Formed by stirring 5.4 mg (13.4 μmol) of $[Rh(COD)_2]^+BF_4^-$ (**4**) and 50.0 mg of SiO_2 for 5 min at room temperature in methanol.
[d] 0.10 ml of Hg added.
[e] See footnote 2.
[f] Oxidized by addition of H_2O_2 to an acetone slurry of the catalyst prior to reaction.
[g] Activity ceases after 10 min.

see footnote 2). Also, mercury quenches the toluene hydrogenation activity of both the palladium and rhodium present in **6** (entry 7).

Oxidation of **6** by reaction with H_2O_2 in acetone at room temperature liberates rhodium from the PPM complex to produce a catalyst that is much more active (TOF = 0.834 min^{-1}) than **6** (entry 8, Table 4). This rate is not much slower than that of the catalyst prepared by adsorbing $[Rh(COD)_2]^+BF_4^-$ (**4**) on Pd-SiO_2 (**7**) (TOF = 1.65 min^{-1}; entry 9). The high activity of rhodium species on Pd-SiO_2 (**7**) is consistent with the previously observed ability of Pd to activate adsorbed rhodium species for arene hydrogenations [18]. Both the oxidized Pd-SiO_2-*R*-PPM-O_2 (**13**) and $[Rh(COD)_2]^+BF_4^-$ (**4**) on Pd-SiO_2 (**7**) catalysts are deactivated when mercury is added to the toluene hydrogenation mixtures. All of these results indicate that a PPM-Rh complex is not active for toluene hydrogenation, but rather metallic rhodium supported on the Pd-SiO_2 (**7**) is the catalyst.

4. Conclusions

4.1. Enantioselective hydrogenation of MAC by SiO_2-R-PPM-Rh-COD (3)

One of the goals of these studies was to characterize the form of the tethered *R*-PPM-Rh-COD (**10**) complex on the silica surface in SiO_2-*R*-PPM-Rh-COD (**3**), before and during the enantioselective hydrogenation of MAC. On silica, the tethered phosphine, SiO_2-*R*-PPM (**2**), is shown to retain the same structure and phosphine environment as in solution, *R*-PPM (**1**). For the tethered metal complex, both Methods A (Scheme 2) and B (Scheme 1) lead to the same SiO_2-*R*-PPM-Rh-COD (**3**) surface species as determined by ^{31}P CPMAS NMR spectroscopy, which also establishes that the Rh complex in SiO_2-*R*-PPM-Rh-COD (**3**) is structurally the same as *R*-PPM-Rh-COD (**10**) in solution. Consistent with the ^{31}P NMR results, the activities and enantioselectivities for the hydrogenation of MAC are the same whether the SiO_2-*R*-PPM-Rh-COD (**3**) catalyst is prepared by either Method A or Method B. The activity of this catalyst is also comparable to that of the homogeneous Rh complex, $[B\text{-PPM-Rh-COD}]^+$, in solution and to that reported earlier by Pugin and Müller [5].

Catalyst **3**, prior to use in MAC hydrogenations, is sensitive to air, undergoing complete oxidation to SiO_2-*R*-PPM-O_2 (**11**) and depositing rhodium on the SiO_2 within 5 days of air exposure or 15 min by reaction with H_2O_2, Eq. (3). Oxidation also occurs at a rate of ∼1% per hour in the NMR rotor used in this study. After use in a MAC hydrogenation, SiO_2-*R*-PPM-Rh-COD (**3**) is extremely air-sensitive and loss of activity is observed within seconds upon exposure to air.

Exposure of solutions containing MAC and the SiO_2-*R*-PPM-Rh-COD (**3**) catalyst to CO before, during, and after hydrogenation produces rhodium CO complexes that exhibit strong ν(CO) IR bands diagnostic of complexes that are formed from intermediates in the catalytic reaction. The identified rhodium-CO complexes are SiO_2-*R*-PPM-Rh-MeOH-CO (**24**) and SiO_2-*R*-PPM-Rh-MAC-CO (**25**). The lack of additional ν(CO) bands shows that the PPM–rhodium complex remains intact throughout the catalytic cycle. Together with solid-state ^{31}P NMR studies, the IR (and DRIFT) results support a previously proposed

mechanism [20,25–31] (Scheme 3) for the hydrogenation of MAC in the presence of **3** and provide evidence that the PPM–rhodium unit remains intact throughout the reaction.

Reaction rates, oxidation experiments, and mercury poisoning experiments reinforce the conclusion that the intact PPM–Rh unit is required for enantioselective hydrogenation of MAC. On silica, excess $[Rh(COD)_2]^+BF_4^-$ (**4**) has no noticeable effect on the rate or enantioselectivity, because $[Rh(COD)_2]^+BF_4^-$ (**4**) by itself is a poor hydrogenation catalyst.[3] Partial oxidation of SiO_2-*R*-PPM-Rh-COD (**3**) to SiO_2-*R*-PPM-O_2 (**11**) reduces its enantioselective activity, while complete oxidation extinguishes it. However, when the PPM–Rh unit remains intact, mercury does not reduce the rate or enantioselectivity of MAC hydrogenation. All of these results suggest that during the hydrogenation of MAC, the phosphine (PPM) remains coordinated to the rhodium throughout the catalytic cycle. Thus, based on ^{31}P NMR and DRIFT spectroscopic studies, as well as investigations of the catalytic activity and enantioselectivities of SiO_2-*R*-PPM-Rh-COD (**3**), it has been established that the active species in catalyst **3** is the tethered *R*-PPM-Rh^+ unit.

4.2. Enantioselective hydrogenation of MAC by Pd-SiO_2-*R*-PPM-Rh-COD (*6*)

When metallic Pd is added to the SiO_2 surface of SiO_2-*R*-PPM-Rh-COD (**3**), the active species of the resulting catalyst Pd-SiO_2-*R*-PPM-Rh-COD (**6**) is also the SiO_2-*R*-PPM-Rh-COD complex. In general, the tethered systems on Pd-SiO_2 (**7**) are similar to those on SiO_2. The tethered phosphine Pd-SiO_2-*R*-PPM (**12**) appears the same by ^{31}P NMR as on silica, SiO_2-*R*-PPM (**2**), and in solution, *R*-PPM (**1**). However, two additional resonances were observed in **12** that most likely represent a complex of *R*-PPM with Pd [24]. Also, Pd-SiO_2-*R*-PPM-Rh-COD (**6**) catalysts, prepared by either Method A or Method B, are similar to each other and to **3**. The spectroscopic data are consistent with the observations that the activities and enantioselectivities of the catalysts (**6** and **3**) with Pd-SiO_2 and SiO_2 supports are very similar. All of the catalysts (**3**A, **3**B, **6**A, and **6**B) catalyze the enantioselective hydrogenation of MAC. Solid-state ^{31}P NMR studies show that the *R*-PPM-Rh-COD complex is the species present in Pd-SiO_2-*R*-PPM-Rh-COD (**6**) prior to the hydrogenation of MAC. Exposure to CO, reaction rates, oxidation experiments, and mercury poisoning experiments indicate that the intact chelated phosphine–rhodium unit is required for enantioselective hydrogenation of MAC and this PPM–Rh unit remains intact throughout the reaction.

In all regards discussed so far, the *R*-PPM-Rh-COD species are the same in **3** and in **6**. The same species are observed before, during, and after reaction; and the Pd-SiO_2 catalyst, **6**, is as air sensitive as **3** on SiO_2. The only difference between the SiO_2- and Pd-SiO_2-supported catalysts is the ability of Pd-SiO_2 (**7**) to activate any uncomplexed rhodium, such as $[Rh(COD)_2]^+BF_4^-$ (**4**), on the silica surface to a highly active racemic hydrogenation species, presumably rhodium metal. Thus, $[Rh(COD)_2]^+BF_4^-$ (**4**) on Pd-SiO_2 (**7**) is reduced to an active form of rhodium that catalyzes the hydrogenation of MAC to the racemic $MACH_2$ product; as noted above, $[Rh(COD)_2]^+BF_4^-$ (**4**) on SiO_2 is not very active (TOF $= 0.0600\,min^{-1}$) for MAC hydrogenation. Therefore, excess $[Rh(COD)_2]^+BF_4^-$ (**4**) on Pd-SiO_2-*R*-PPM-Rh-COD (**6**) results in reduced enantioselectivities due to concurrent enantioselective and racemic hydrogenation by the two different species. Also, oxidation of Pd-SiO_2-*R*-PPM-Rh-COD (**6**) releases rhodium species that are reduced by the Pd under hydrogenation conditions to rhodium metal which causes the hydrogenation of MAC to give lower ee values in the $MACH_2$ product. For all of the catalysts containing Pd-SiO_2, mercury quenches the part of the reaction catalyzed by metallic rhodium that gives racemic $MACH_2$ yet allows the enantioselective hydrogenation catalyzed by the *R*-PPM-Rh-COD complex.

4.3. Arene hydrogenation by SiO_2-*R*-PPM-Rh-COD (*3*) and Pd-SiO_2-*R*-PPM-Rh-COD (*6*)

Although several catalysts consisting of a thethered Rh complex on Pd-SiO_2 are active for the hydrogenation of arenes [7–11], catalysts described in this

[3] $[Rh(COD)_2]^+BF_4^-$ in solution and on SiO_2 is a poor hydrogenation catalyst, see Table 2, entry 7 and Table 4, entry 1. While the reduced rhodium metal is highly active, the reduction of $[Rh(COD)_2]^+BF_4^-$ to rhodium metal is slow under reaction conditions, taking days at 40 °C [18].

paper, based on *R*-PPM-Rh-COD (**10**), are not. While SiO_2-*R*-PPM-Rh-COD (**3**) shows trace activity for toluene hydrogenation, the mercury test shows conclusively that the activity cannot be ascribed to the PPM–Rh complex; rather metallic rhodium on the silica is the active species. Somewhat surprisingly, the TCSM catalyst, Pd-SiO_2-*R*-PPM-Rh-COD (**6**), does not show an increase in toluene hydrogenation activity over that of Pd-SiO_2 (**7**), which suggests that the Pd-SiO_2 part of **6** is the active component. When **6** is oxidized to Pd-SiO_2-*R*-PPM-O_2 (**13**) releasing Rh from the complex, toluene hydrogenation activity increases substantially. After extensive oxidation, the rate is the same as that of $[Rh(COD)_2]^+BF_4^-$ (**4**) on Pd-SiO_2 (**7**). This increased toluene hydrogenation activity corresponds with reduced enantioselectivities for MAC hydrogenation. Most importantly, mercury stops both the toluene and the racemic MAC hydrogenation activity. This indicates that these activities are due to rhodium metal and not the PPM–Rh complex. Again, the difference in arene hydrogenation activity between $[Rh(COD)_2]^+BF_4^-$ (**4**) on Pd-SiO_2 (**7**), which is highly active (TOF $= 1.65\,min^{-1}$), and $[Rh(COD)_2]^+BF_4^-$ (**4**) on SiO_2, which is much less active (TOF $= 0.0604\,min^{-1}$), is due to Pd facilitating the reduction of $[Rh(COD)_2]^+BF_4^-$ (**4**) to a form of rhodium metal that is the active toluene hydrogenation species. For all of the catalysts examined with the PPM ligand, the intact tethered catalyst is inactive for arene hydrogenation.

Acknowledgements

This research was supported at Ames Laboratory by the US Department of Energy, Office of Science, Office of Basic Energy Sciences, Division of Chemical Sciences, under Contract W-7405-Eng-82 with Iowa State University.

References

[1] J.D. Morrison (Ed.), Asymmetric Synthesis, vol. 5, Chiral Catalysis, Academic Press, Orlando, 1985.
[2] D.E. Vos, I.F.J. Vankelecom, P.A. Jacobs (Eds.), Chiral Catalyst Immobilization and Recycling, Wiley, New York, 2000.
[3] E.N. Jacobsen, A. Pfaltz, H. Yamamoto (Eds.), Comprehensive Asymmetric Catalysis, vols. 1 and 3, Springer, New York, 1999.
[4] M.J. Burk, F. Bienewald, Transition Met. Org. Synth. 2 (1998) 13.
[5] B. Pugin, M. Müller, in: M. Guisnet, et. al. (Eds.), Stud. Surf. Sci. Cat. Part 78: Heterogeneous Catalysis and Fine Chemicals III, Elsevier, 1993, p. 107.
[6] B. Pugin, J. Mol. Catal. A: Chem. 107 (1996) 273.
[7] H. Gao, R.J. Angelici, J. Mol. Catal. A: Chem. 149 (1999) 63.
[8] H. Gao, R.J. Angelici, J. Am. Chem. Soc. 119 (1997) 6937.
[9] H. Gao, R.J. Angelici, Organometallics 18 (1999) 989.
[10] H. Gao, R.J. Angelici, New J. Chem. 23 (1999) 633.
[11] H. Yang, H. Gao, R.J. Angelici, Organometallics 19 (2000) 622.
[12] A.B. Pangborn, M.A. Giardello, R.H. Grubbs, R.K. Rosen, F.J. Timmers, Oganometallics 15 (1996) 1518.
[13] D.D. Perrin, W.L.F. Armarego, D.R. Perrin, Purification of Laboratory Chemicals, 2nd ed., Pergamon Press, New York, 1980.
[14] J. Suh, E. Lee, Y.C. Myoung, M. Kim, S. Kim, J. Org. Chem. 50 (1985) 977.
[15] R.M. Herbst, D. Shemin, in: A.H. Blatt (Ed.), Organic Syntheses, Collect. vol. 2, Wiley, New York, 1943, p. 1.
[16] R.R. Schrock, J.A. Osborn, J. Am. Chem. Soc. 93 (1971) 3089.
[17] T. Ioannides, X. Veeykios, J. Catal. 140 (1993) 353.
[18] K.J. Stanger, Y. Tang, J. Anderegg, R.J. Angelici, in preparation.
[19] S. Hediger, B.H. Meier, R.R. Ernst, J. Chem. Phys. 102 (1995) 4000.
[20] I. Ojima, T. Kogure, N. Yoda, J. Org. Chem. 45 (1980) 4728.
[21] K. Achiwa, P.A. Chaloner, D. Parker, J. Organomet. Chem. 218 (1981) 249.
[22] M.A. Garralda, L.A. Oro, Transition Met. Chem. 5 (1980) 63.
[23] M. Green, T.A. Kuc, S.H. Taylor, J. Chem. Soc. A (1971) 2334.
[24] Note the presence of two resonances at around 40 and 20 ppm in the spectrum of Fig. 1d. The fact that these resonances were not observed in the corresponding spectrum of sample **2**, indicates a complex of *R*-PPM with Pd. However, on addition of $[Rh(COD)_2]^+BF_4^-$ these signals disappear, Fig. 1f, indicating that any (PPM-Pd) complex is only weakly bound.
[25] J.Halpern.D.P. Riley, A.S.C. Chan, J.J. Pluth, J. Am. Chem. Soc. 99 (1977) 8055.
[26] A.S.C. Chan, J. Halpern, J. Am. Chem. Soc. 102 (1980) 838.
[27] A.S.C. Chan, J.J. Pluth, J. Halpern, J. Am. Chem. Soc. 102 (1980) 5952.
[28] (a) C.R. Landis, J. Halpern, J. Organomet. Chem. 250 (1983) 485;
(b) C.R. Landis, J. Halpern, J. Am. Chem. Soc. 109 (1987) 1746.
[29] (a) I.D. Grdnev, N. Higashi, K. Asakura, T. Imamoto, J. Am. Chem. Soc. 122 (2000) 7194;
(b) I.D. Grdnev, N. Higashi, T. Imamoto, J. Am. Chem. Soc. 123 (2001) 4631.

[30] (a) C.R. Landis, P. Hilfenhaus, S. Feldgus, J. Am. Chem. Soc. 121 (1999) 8741;
(b) S. Feldgus, C.R. Landis, J. Am. Chem. Soc. 122 (2000) 12714;
(c) S. Feldgus, C.R. Landis, Organometallics 20 (2001) 2374.
[31] J.P. Collman, L.S. Hegedus, J.R. Norton, R.G. Finke, Principles and Applications of Organotransition Metal Chemistry, University Science Books, Mill Valley, CA, 1987.
[32] R.R. Schrock, J.A. Osborn, J. Am. Chem. Soc. 93 (1971) 2397.
[33] A.D. Zotto, L. Costella, A. Mezzetti, P. Rigo, J. Organomet. Chem. 414 (1991) 109.
[34] L.M. Haines, Inorg. Chem. 10 (1971) 1693.
[35] M.P. Keyes, K.L. Watters, J. Catal. 110 (1988) 96.
[36] C.R. Guerra, J.H. Schulman, Surface Science 7 (1967) 229.
[37] S.D. Worley, C.A. Rice, G.A. Mattson, C.W. Curtis, J.A. Guin, A.R. Tarrer, J. Phys. Chem. 86 (1982) 2714.
[38] C.A. Rice, S.D. Worley, C.W. Curtis, A.J. Guin, A.R. Tarrer, J. Chem. Phys. 74 (1981) 6487.
[39] K.S. Weddle, J.D. Aiken III, R.G. Finke, J. Am. Chem. Soc. 120 (1998) 5653.
[40] G. Webb, J.I. Macnab, J. Catal. 26 (1972) 226.